



**Active Nonmetallic Au and Pt Species on
Ceria-Based Water-Gas Shift Catalysts**

Qi Fu, *et al.*

Science **301**, 935 (2003);

DOI: 10.1126/science.1085721

**The following resources related to this article are available online at
www.sciencemag.org (this information is current as of September 11, 2007):**

Updated information and services, including high-resolution figures, can be found in the online version of this article at:

<http://www.sciencemag.org/cgi/content/full/301/5635/935>

Supporting Online Material can be found at:

<http://www.sciencemag.org/cgi/content/full/1085721/DC1>

This article **cites 16 articles**, 1 of which can be accessed for free:

<http://www.sciencemag.org/cgi/content/full/301/5635/935#otherarticles>

This article has been **cited by** 213 article(s) on the ISI Web of Science.

This article has been **cited by** 3 articles hosted by HighWire Press; see:

<http://www.sciencemag.org/cgi/content/full/301/5635/935#otherarticles>

This article appears in the following **subject collections**:

Chemistry

<http://www.sciencemag.org/cgi/collection/chemistry>

Information about obtaining **reprints** of this article or about obtaining **permission to reproduce this article** in whole or in part can be found at:

<http://www.sciencemag.org/about/permissions.dtl>

Active Nonmetallic Au and Pt Species on Ceria-Based Water-Gas Shift Catalysts

Qi Fu, Howard Saltsburg, Maria Flytzani-Stephanopoulos*

Traditional analysis of reactions catalyzed by supported metals involves the structure of the metallic particles. However, we report here that for the class of nanostructured gold- or platinum-ceria catalysts, which are active for the water-gas shift reaction, metal nanoparticles do not participate in the reaction. Nonmetallic gold or platinum species strongly associated with surface cerium-oxygen groups are responsible for the activity.

The heterogeneously catalyzed water-gas-shift (WGS) reaction ($\text{CO} + \text{H}_2\text{O} \leftrightarrow \text{CO}_2 + \text{H}_2$) is a key step in fuel processing to generate H_2 . Such heterogeneous catalysts should combine both high activity and structural stability in air and in cyclic operation; these are stringent requirements not met by the commercially available low-temperature WGS catalysts. A new class of WGS catalysts based on cerium oxide (ceria) has been investigated extensively in recent years (1–6). To provide low-temperature WGS activity, Pt-group metals (PM), Au, or Cu are suitably added in amounts that vary from ~1 to 10 weight percent (wt %). A critical problem with Pt-ceria catalysts is their prohibitive economics (3), due to the cost of Pt, even if their issues of deactivation with time-on-stream are resolved. However, ceria containing only trace amounts of Pt would be economical. Similarly attractive would be ceria containing base metals or oxides. We have reported recently that an excellent shift catalyst results from supporting Au or Cu on nanocrystalline ceria (4–6). This type of catalyst, if properly developed, would of course be much more economical, i.e., practical for large-scale fuel cell application. We show here that low loadings of metal can be as effective as much higher loadings.

The PM-ceria catalysts have received considerable attention because of their use in the automobile catalytic converter (7, 8). It is widely accepted that the oxygen in ceria plays an important role in the reaction pathway (1, 4, 9). However, identification of the active sites for low-temperature CO oxidation, the WGS reaction, and other oxidation reactions on PM-ceria catalysts remains an issue of contention. In most reports, the active sites are placed at the metal-ceria interface (1, 9), whereas in others Pt ions dispersed on the surface of ceria are as-

sumed to be active (10). Encapsulation of Pt by reduced ceria nanoparticles has also been proposed (11).

In the work reported here, all catalyst components were nanocrystalline. Nanocrystalline ceria can be prepared by various techniques (2, 4). Ceria particles with diameters of less than 10 nm have markedly higher electronic conductivity over that of centered ceria (12), and doping with a rare earth oxide, such as La_2O_3 , can be used to create oxygen vacancies and to stabilize ceria particles against sintering (13). We prepared such nanosized La-doped ceria and deposited Au or Pt on it. After thermal annealing, these materials had excellent and as-yet-unexplained properties for the low-temperature WGS reaction. Au or Pt exists as nanosized particles and in ionic state in these catalysts. The catalytic activity was not affected by the removal of metallic Au or Pt particles by cyanide leaching. Thus, metallic nanoparticles are not necessary for the activity; they are mere spectators in the WGS reaction. Nonmetallic Au or Pt species embedded in ceria catalyze the reaction of CO with H_2O .

We prepared most of the Au-ceria catalysts by the same technique; ceria (doped with 10 atom % La) was synthesized by urea gelation/coprecipitation (UGC) (4) and then calcined in air at 400°C for 10 hours. This treatment produced ceria with a mean particle size of ~5 nm (5), with a surface area of ~150 m²/g. Au was then applied onto ceria by deposition-precipitation (DP) (5) at room temperature, through dropwise addition of HAuCl_4 into a suspension of the ceria particles in an aqueous solution of $(\text{NH}_4)_2\text{CO}_3$ at a constant pH (~8). After several washes and drying, the Au-ceria particles were calcined in air at 400°C for 10 hours. Most of the Au thus prepared was in the form of metal nanoparticles with an average size of ~5 nm (5, 6). The deposition step had a negligible effect on the total surface area of ceria. For comparison, we prepared a Au-ceria sample by a single

coprecipitation (CP) step. This involved mixing an aqueous solution of HAuCl_4 , $\text{Ce}(\text{NO}_3)_3$, and $\text{La}(\text{NO}_3)_3$ with $(\text{NH}_4)_2\text{CO}_3$ at 60° to 70°C, keeping it at a constant pH (~8), and aging the precipitate at the same temperature for 1 hour. Leaching of gold took place in an aqueous solution of 2% NaCN at room temperature. Sodium hydroxide was added to keep the pH at ~12. [This same process is used to extract gold during gold mining (14).] No Ce or La was found in the leachate. The leached samples were washed, dried (at 120°C for 10 hours), and heated in air (at 400°C for 2 hours). More than 90% of the Au loading was removed from the ceria by this leaching procedure. Scanning transmission electron microscopy and energy-dispersive x-ray spectroscopy showed no Au particles remaining, only what appeared to be very fine clusters or atomically dispersed Au. X-ray photoelectron spectroscopy (XPS) identified ionic Au as the major or only Au species present in the leached materials (Fig. 3A).

A similar procedure was used to remove excess Pt from the ceria surface. First, Pt-ceria was prepared by incipient wetness impregnation (IMP). La-doped ceria (CL) powders were prepared by UGC as described above. They were then impregnated with an aqueous solution of H_2PtCl_6 of appropriate concentration, the volume of which equaled the total pore volume of ceria. After impregnation, the samples were degassed and dried at room temperature under vacuum. After drying in a vacuum oven at 110°C for 10 hours, the samples were crushed and calcined in air at 400°C for 10 hours. Calcined Pt-ceria samples were leached by the same procedure as the Au catalysts; the leached sample is denoted as Pt-CL(IMP, NaCN1). To further reduce the amount of Pt, Pt-CL(IMP, NaCN1) was leached in a 2% NaCN solution at 80°C for 12 hours. The corresponding sample is denoted as Pt-CL(IMP, NaCN2). The properties of the thus-prepared Au- and Pt-ceria samples are presented in Table 1.

Arrhenius-type plots of the WGS reaction rate measured over the as-prepared Au-ceria catalysts and the Au-free ceria (CL) are shown in Fig. 1. The reacting gas mixture simulates a reformat gas composition: 11% CO, 7% CO_2 , 26% H_2 , and 26% H_2O , in an inert gas carrier. Activation of catalysts was not necessary (15). Similar rates of CO_2 production (per square meter of catalyst surface area) were measured over the parent [4.4 (CP), 4.7 (DP), or 2.8 (DP) atom % Au] and the corresponding leached (0.7, 0.44, or 0.23 atom % Au) ceria catalysts. The apparent activation energy (E_a) for the reaction was the same for parent and leached catalysts: 47.8 ± 1.5 kJ/mol for the DP samples and 36.8 ± 0.9 kJ/mol for the CP samples. The rate over the nanosized CL sample was much lower than

Department of Chemical and Biological Engineering, Tufts University, Medford, MA 02155, USA.

*To whom correspondence should be addressed. E-mail: maria.flytzani-stephanopoulos@tufts.edu

REPORTS

Table 1. Physical properties of ceria-based catalysts. All samples were calcined at 400°C; CL is Ce(10 atom % La)O_x, calcined at 400°C, for 10 hours. Numbers in sample names represent atom %. NM, not measured; ND, not detectable; NA, not applicable.

Sample	Surface area (m ² /g)	Surface metal content* (atom %) Au or Pt	Bulk composition (atom %) [†]			Particle size [‡] (nm)			
			Metal (Au or Pt)	Ce	La	Metal (Au or Pt)	CeO ₂		
							<111>	<220>	
4.7 Au-CL (DP)	156.1	1.60	4.71	87.88	7.41	5.0	5.2	4.9	
0.4 Au-CL (DP) (NaCN)	157.9	0.61	0.44	91.24	8.32	ND	5.2	4.9	
2.8 Au-CL (DP)	159.2	1.58	2.81	89.16	8.03	4.7	5.0	4.9	
0.2 Au-CL (DP) (NaCN)	162.2	0.43	0.23	93.10	6.67	ND	5.0	4.9	
3.4 Au-CeO ₂ § (DP)	25.9	NM	3.36	96.64	0	4.0	21.1	20.3	
0.001 Au-CeO ₂ (DP)§ (NaCN)	28.0	NM	~0.001	~99.999	0	ND	21.0	20.4	
CL (UGC)	156.9	NA	0	92.62	7.38	NA	5.1	4.8	
4.4 Au-CL (CP)	47.8	3.29	4.35	88.00	7.65	12.9	7.2	6.3	
0.7 Au-CL (CP) (NaCN)	47.5	0.24	0.67	91.52	7.82	ND	7.0	6.0	
3.7 Pt-CL (IMP)	129.8	1.63	3.67	88.83	7.50	2.5	6.2	6.1	
2.7 Pt-CL (IMP, NaCN1)	147.5	1.79	2.70	89.78	7.52	ND	6.2	6.1	
1.5 Pt-CL (IMP, NaCN2)	103.2	0.82	1.50	90.86	7.64	ND	6.2	6.1	

*Surface metal content was determined by XPS. [†]Bulk composition was determined by ICP. [‡]Particle size was determined by XRD with the Scherrer equation. [§]CeO₂ was calcined at 800°C. ||Particle size was determined by HRTEM.

the Au-containing CL over the temperature range of interest, with an E_a of 83 kJ/mol. Fig. 1 also shows the rate measured over a commercial Cu-ZnO-Al₂O₃ (United Catalysts Inc., G-66A) low-temperature WGS catalyst, which contains 42 wt % Cu. Although the rate was greater over this catalyst, its use in fuel cell applications is highly unlikely because of its air sensitivity and its narrow operating temperature window. Moreover, a careful activation in H₂ is required for Cu/ZnO catalysts. However, ceria-based WGS catalysts require no activation and are not air-sensitive.

The reaction pathway on the Au-ceria catalysts was different from that on Au-free ceria (Fig. 1). Also, only the Au species present on the leached catalyst must be associated with the active sites, because the extra Au present in the parent material did not increase the rate; nor did it change the E_a for the reaction. If we assume complete dispersion of Au in the leached catalysts, we can calculate the turnover frequency (TOF) from the data in Fig. 1. For example, at 300°C, the TOF is 0.65 molecules of CO₂ per Au atom per second.

In kinetic studies with the Pt-ceria catalysts (16) (fig. S1), the E_a over the parent (3.7 atom % Pt) and the leached Pt-ceria (2.7 or 1.5 atom % Pt) was the same, 74.8 ± 0.6 kJ/mol. The WGS rate over these samples was similar. The isokinetic temperature for the Pt- and Au-ceria (DP) samples is 250°C. Transient light-off curves for the WGS reaction over the Pt-ceria catalysts (Fig. 2) were collected in temperature-programmed reaction mode. These profiles were reproduced after samples were cooled down from the high end-point temperature and the transient test was repeated. The light-off temperature was lowest for the catalyst that contained the lowest amount of Pt (by leaching). Thus, the removed Pt was not important for the reac-

Fig. 1. WGS rates measured in a reformate-type gas composed of 11% CO, 7% CO₂, 26% H₂, 26% H₂O, and balance He [see Table 1 for sample properties, (15) for details]. Solid squares, 4.4 atom % AuCe(La)O_x (CP); open squares, 0.7 atom % AuCe(La)O_x (CP, leached); solid triangles, 4.7 atom % AuCe(La)O_x (DP); open triangles, 0.44 atom % AuCe(La)O_x (DP, leached); solid circles, 2.8 atom % AuCe(La)O_x (DP); open circles, 0.23 atom % AuCe(La)O_x (DP, leached); asterisks, Ce(La)O_x; diamonds, G-66A (42 wt % CuO, 47 wt % ZnO, 10 wt % Al₂O₃, surface area 49 m²/g). T(1/K), temperature in Kelvin.

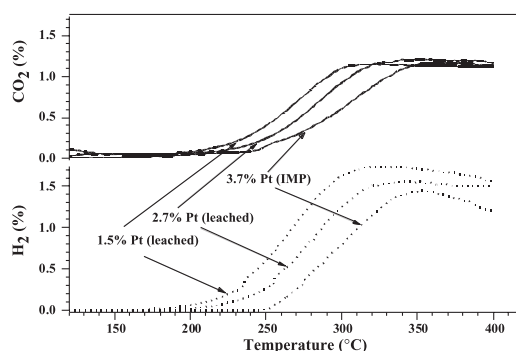
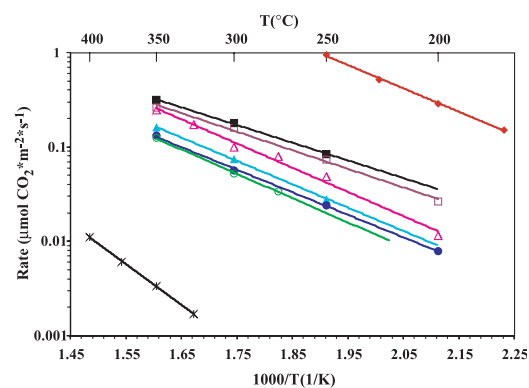


Fig. 2. Temperature-programmed reaction of as-prepared and leached Pt-ceria catalysts in a 2% CO-3% H₂O-He gas (see Table 1 for sample properties).

tion, and the leaching process must have increased the number of active sites.

The oxidation states of Au and Pt in both the parent and leached ceria samples were checked by XPS (Fig. 3). The common features in both systems were (i) the existence of ionic states (Au^{+1,+3} and Pt^{+2,+4}) both before and after leaching, and (ii) the complete removal of metallic Au or Pt nanoparticles after the leaching step. No Ce or La loss took place during the leaching step, as verified by inductively coupled plasma (ICP) analysis of the leachate solutions. The absence of Au or Pt particles on the leached ceria samples was

also confirmed by high-resolution transmission electron microscopy (HRTEM). The intensities shown in Fig. 3A cannot be used to compare the amounts of Au between parent and leached samples. In fact, the surface metal content of the parent DP and CP samples was grossly underestimated (Table 1), because average metal particle sizes greatly exceeded the electron escape depth. The agreement is better for the leached Au-ceria samples. Finally, all Pt-ceria samples show much less Pt on the surface than expected on the basis of the ICP analysis and the surface area of each sample. In both Au- and Pt-ceria,

Fig. 3. X-ray photoelectron spectra of as-prepared and leached samples. (A) Au-ceria. (B) Pt-ceria [see Table 1 for sample properties, (17) for comments]. X5 and X25 represent signal magnification.

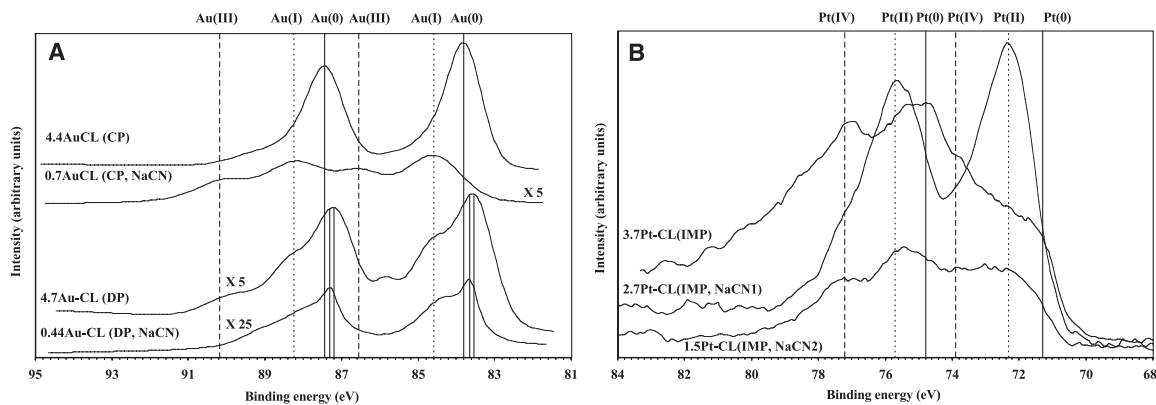
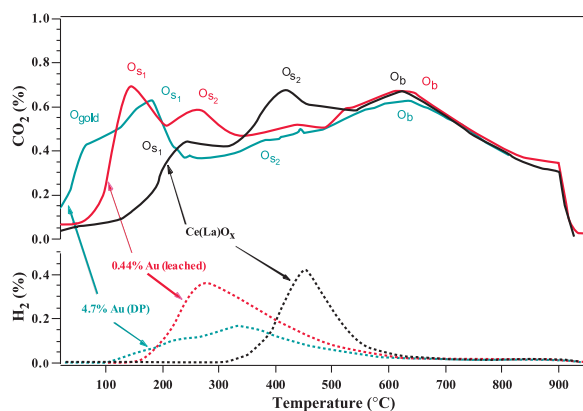


Fig. 4. CO-TPR profiles of as-prepared and leached Au-CL (DP) and CL samples; 10 mole % CO in He, 50 cm³ per min [see Table 1 for sample properties, (24) for details].



diffusion of Au or Pt ions into subsurface layers of ceria is plausible.

The 4.4 atom % Au-CL catalyst prepared by CP shows Au⁰ binding energies at 83.8 and 87.4 eV; this sample contains metallic Au particles with a mean size of 12.2 nm (Table 1). Leaching removed all metallic gold (Fig. 3A) for the 0.7 atom % Au-CL sample. Both Au⁺¹ and Au⁺³ were present in the leached sample. The 4.7 atom % Au-CL catalyst prepared by DP shows Au⁰ lines as well as ionic Au. The corresponding leached material shows ionic Au binding energies, as well as a positively shifted (by ~0.1 eV) binding energy of Au⁰. This shift is within the experimental error of the analysis. Deconvolution of the spectra shows that the zerovalent species amount to only 14% of the total Au present in the leached 0.44 atom % Au-CL sample (Fig. 3A) (17–19).

It may be argued that the oxidic Au observed in our samples is due to the preparation conditions (air calcination at 400°C), and that during reaction under net reducing conditions, zerovalent Au would dominate. This possibility would require further studies. An important observation, however, is that the used catalyst, after more than 20 hours at reaction conditions, cannot be further leached; i.e., even if Au changes oxidation state during reaction, it does not migrate to form metallic particles. XPS analysis of Au-ceria catalysts after 15 hours of use in the reaction gas mixture in Fig. 1 showed

predominance of ionic Au (16) (fig. S2). The Au-O-Ce structures are stable under the conditions in this work. Similar arguments can be made for the Pt-ceria catalysts. For this type of material, surface Pt-O phases strongly associated with ceria have been reported (10).

The use of dry CO in temperature-programmed reduction (TPR) (CO-TPR) identified oxygen species of importance to the low-temperature WGS reaction on the parent and leached catalysts. Various types of oxygen have been identified on ceria (20, 21), ranging from weakly bound adsorbed oxygen to surface capping oxygen to lattice oxygen, depending on the operating temperature. A synergistic redox model for metal-CeO₂ has been proposed, in which the metal particle participates by providing adsorption sites for CO (1, 4, 22, 23), while ceria supplies the required oxygen. This simple model does not provide atomic-level understanding and mechanistic resolution of several key questions; most importantly, it assigns the CO adsorption sites on metal particles. However, as Figs. 1 and 2 show, the WGS activity of metal-free (leached) ceria is similar to that of the metal-containing samples.

CO-TPR (24) results from fully oxidized parent and leached Au-ceria (DP) samples and from the CL material are shown in Fig. 4. The first CO₂ peak produced on the parent Au-ceria sample is absent in the leached sample and in the Au-free, CL material. This

peak is thus assigned to oxygen adsorbed on metallic Au nanoparticles, which are present only on the parent 4.7 atom % Au-CL sample. The high-temperature oxygen species, O_b, is of similar reducibility in all three samples. Thus, the presence of Au did not affect the bulk (lattice) oxygen of ceria. However, the reducibility of the surface oxygen species of ceria, O_{s1} and O_{s2}, was greatly increased for both Au-containing samples (Fig. 4). This result correlates well with the markedly higher WGS activity of the Au-CL catalyst compared to that of the CL material shown in Fig. 1.

The appearance of H₂ along with CO₂ elution during CO-TPR is attributed to surface hydroxyls that remain in ceria even after the oxidation pretreatment step in a dry O₂/He mixture at 350°C (2). Indeed, when we repeated the CO-TPR after reoxidation at 400°C, very little H₂ was produced, and by the fourth cycle, only trace amounts of H₂ evolved. The amount of CO₂ eluted in all cycles was the same, and its production began and peaked at the same temperatures as those shown for the first cycle in Fig. 4. A higher amount of CO₂ was eluted from the leached catalyst (Fig. 4, the area under the O_{s1} peak). This difference may be due to unmasking of sites after the metallic particles that cover them are leached away.

How do Au ions or adatoms interact with ceria to weaken both its O_{s1} and O_{s2} surface oxygens? A distribution of electronic charges between atomic Au or a small cluster of Au atoms and ceria could weaken the Ce-O bond. Evidence from H₂-TPR and separate pulse reactor experiments with CO in our lab (6) strongly suggests that Au increases the amount of surface oxygen in ceria. This increase can occur through partial lattice filling of vacant Ce sites with Au^{δ+}, which would create additional oxygen vacancies on the surface of the Ce⁴⁺-O₂ fluoride-type oxide.

The identification of Au ions (Fig. 3A), along with the increased amount of surface oxygen in the leached sample (Fig. 4), argues in favor of lattice substitution. Diffusion of Au ions into ceria must take place during the heat-

REPORTS

ing step in the preparation process, because attempts to leach the Au immediately after deposition and before heating failed to produce an active catalyst. The minimum metal loading required for a desired WGS activity may be determined from the ceria surface properties. Assuming uniform, monolayer, dimensioned metal surface coverage on the CL material [Ce(10 atom % La)O_x, 160 m²/g], we calculated the coverage to be 13.5 atom % Au or 15.5 atom % Pt, with the Au or Pt radius equal to 0.174 nm and 0.139 nm, respectively. Only a small fraction of a monolayer of Au or Pt was present on the leached catalysts (Table 1 and Figs. 1 and 2), but this amount correlates well with the concentration of surface oxygen defect sites of ceria (25–27).

The importance of the surface defects of ceria as the anchoring sites of Au, and in turn as the active sites for the WGS reaction, can be seen in ceria samples annealed at high temperatures, which effectively reduces the number density of these sites. The reaction rate measured over 3.4 atom % Au-CeO₂ (calcined at 800°C for 4 hours) (Table 1) was very low, but the apparent activation energy was the same as for the other Au-ceria (DP) materials shown in Fig. 1. Removal of Au from this sample by leaching was essentially complete (Table 1) and the leached sample was inactive for the WGS reaction up to 400°C.

Au nanoparticles are essential for some oxidation reactions, in view of their totally different oxygen adsorption properties compared with those of bulk Au (28, 29). However, they are unimportant in the WGS reaction over Au-ceria.

References and Notes

1. T. Bunluesin, R. J. Gorte, G. W. Graham, *Appl. Catal. B* **15**, 107 (1998).
2. S. L. Swartz, M. M. Seabaugh, C. T. Holt, W. J. Dawson, *Fuel Cell Bull.* **30**, 7 (2001).
3. J. M. Zalc, V. Sokolovskii, D. G. Loffler, *J. Catal.* **206**, 169 (2002).
4. Y. Li, Q. Fu, M. Flytzani-Stephanopoulos, *Appl. Catal. B* **27**, 179 (2000).
5. Q. Fu, A. Weber, M. Flytzani-Stephanopoulos, *Catal. Lett.* **77**, 87 (2001).
6. Q. Fu, S. Kudriavtseva, H. Saltsburg, M. Flytzani-Stephanopoulos, *Chem. Eng. J.* **93**, 41 (2003).
7. H. S. Gandhi, A. G. Piken, M. Shelef, R. G. Delosh, *SAE Tech. Papers* **55**, 760201 (1976).
8. M. Shelef, G. W. Graham, R. W. McCabe, in *Catalysis by Ceria and Related Materials*, A. Trovarelli, Ed., Catalytic Science Series, vol. 2 (Imperial College Press, London, 2002), pp. 343–376.
9. A. Trovarelli, *Catal. Rev. Sci. Eng.* **38**, 439 (1996).
10. L. L. Murrell, S. J. Tauster, D. R. Anderson, in *Catalysis and Automotive Pollution Control II*, A. Cruick, Ed. (Elsevier, Amsterdam, 1991), pp. 275–289.
11. C. Hardacre, R. M. Ormerod, R. M. Lambert, *J. Phys. Chem.* **98**, 10901 (1994).
12. Y. M. Chiang, E. B. Lavik, I. Kosacki, H. L. Tuller, J. Y. Ying, *J. Electroceramics* **1**, 7 (1997).
13. J. Kaspar, M. Graziani, P. Fornasiero, in *Handbook on the Physics and Chemistry of Rare Earths: The Role of Rare Earths in Catalysis*, K. A. Gschneidner Jr., L. Eyring, Eds. (Elsevier, Amsterdam, 2000), pp. 159–267.
14. N. Hedley, H. Tabachnik, *Chemistry of Cyanidation* (American Cyanamid Company, Wayne, NJ, 1968).
15. After heating in He to the desired temperature, the

- reaction gas mixture was introduced in a flow micro-reactor that contained a packed-bed of catalyst particles (<50 μm in size). Rates were measured for 2 hours at each temperature, and only steady-state data are reported. Measurements were conducted with the same catalyst charge in descending temperature mode; upon completion of the series of runs, the rate was measured again at 300°C. The new value was within 5% of the initial rate at this temperature.
16. Materials and methods are available as supporting material on Science Online.
17. Initial- and final-state effects on the binding energy of Au clusters on ceria are not available in the literature. Generally, final-state effects cause a positive shift of the binding energy of metallic nanoparticles as their size is decreased (18), but below a certain cluster size (~2 nm), initial-state effects prevail (19), causing negative binding energy shifts. Therefore, extensive compensation effects are possible. The observed minor, positive energy shift may be due to partially oxidized Au clusters.
18. C. R. Henry, *Surf. Sci. Rep.*, **31**, 235 (1998).
19. J. Radnik, C. Mohr, P. Claus, *Phys. Chem. Chem. Phys.* **5**, 172 (2003).
20. C. Li, K. Domen, K. I. Maruya, T. Onishi, *J. Catal.* **123**, 436 (1990).
21. R. Q. Long, Y. P. Huang, H. L. Wan, *J. Raman Spectrosc.* **28**, 531 (1997).
22. W. Liu, M. Flytzani-Stephanopoulos, *J. Catal.* **153**, 304 (1995).
23. W. Liu, M. Flytzani-Stephanopoulos, *J. Catal.* **153**, 317 (1995).
24. CO-TPR was carried out in a Micromeritics Pulse ChemiSorb 2705 instrument. The samples were first oxidized in a 10 mole % O₂ in He gas mixture [50 cm³/min normal temperature and pressure (NTP)] at 350°C for 90 min, then cooled down to room temperature and purged with pure He (Grade 5) for 30 min. A 10 mole % Co in He gas mixture [50 cm³/min (NTP)] was passed over the sample, which was heat-

ed at 5°C per min to 900°C. The effluent gas was analyzed by mass spectrometry (MKS model RS-1). The cyclic CO-TPR experiments were conducted only up to 400°C to avoid structural changes in the catalyst at higher temperatures.

25. Defects in ceria are of two types, intrinsic or extrinsic (26). Intrinsic defects are due to the oxygen anion vacancies created by thermal disorder or by the reduction of ceria (26). The extrinsic defects are due to oxygen anion vacancies created by the charge compensation effect of lower valence foreign cations (26). The concentration of defects can be calculated from the lattice expansion measured by x-ray diffraction (XRD) (27). If we assume that Au only associates with the oxygen defects in ceria, the required Au (or Pt) is 0.13 atom % for undoped CeO₂ and 0.57 atom % for Ce(10 atom % La)O_x (both calcined at 400°C), and only 0.03 atom % for the undoped CeO₂ calcined at 800°C (Table 1). These values will increase if Au or Pt ions substitute in the ceria lattice.
26. H. L. Tuller, A. S. Nowick, *J. Electrochem. Soc.* **126**, 209 (1979).
27. J. R. McBride, K. C. Hass, B. D. Poindexter, W. H. Weber, *J. Appl. Phys.* **76**, 2435 (1994).
28. M. Valden, X. Lai, D. W. Goodman, *Science* **281**, 1647 (1998).
29. V. A. Bondzie, S. C. Parker, C. T. Campbell, *Catal. Lett.* **63**, 143 (1999).
30. We gratefully acknowledge the support of this work by the National Science Foundation and the U.S. Environmental Protection Agency, under grant no. CTS 9985305.

Supporting Online Material

www.sciencemag.org/cgi/content/full/1085721/DC1
Figs. S1 and S2

15 April 2003; accepted 18 June 2003
Published online 3 July 2003;
10.1126/science.1085721
Include this information when citing this paper.

A Possible Primordial Peptide Cycle

Claudia Huber,¹ Wolfgang Eisenreich,¹ Stefan Hecht,¹
Günter Wächtershäuser^{2*}

α-Amino acids can undergo peptide formation by activation with carbon monoxide (CO) under hot aqueous conditions in the presence of freshly coprecipitated colloidal (Fe,Ni)S. We now show that CO-driven peptide formation proceeds concomitantly with CO-driven, N-terminal peptide degradation by racemizing N-terminal hydantoin and urea derivatives to α-amino acids. This establishes a peptide cycle with closely related anabolic and catabolic segments. The hydantoin derivative is a purin-related heterocycle. The (Fe,Ni)S-dependent urea hydrolysis could have been the evolutionary precursor of the nickel-enzyme urease. The results support the theory of a chemoautotrophic origin of life with a CO-driven, (Fe,Ni)S-dependent primordial metabolism.

Extant metabolisms depend on cyclic protein turnover with anabolic condensation and catabolic degradation segments. In a primordial organism, the proteins would have been preceded by peptides, but a cyclic turnover from amino acids to peptides and back to amino

acids should already have been operative. Otherwise, functionless peptides would have been futile sinks for valuable amino acids. Previously, we demonstrated the anabolic segment from amino acids to peptides, driven by CO in the presence of coprecipitated (Fe, Ni)S and Na₂S (1). We have now investigated the course of the catabolic segment from peptides back to amino acids.

Experiments for testing CO-driven peptide formation in the presence of (Fe,Ni)S and Na₂S are complicated by a pH problem. CO is continuously hydrated to HCOOH and ox-

¹Department for Organic Chemistry and Biochemistry, Technische Universität München, Lichtenbergstraße 4, D-85747 Garching, Germany. ²Tal 29, D-80331 München, Germany.

*To whom correspondence should be addressed. E-mail: info@patent.de